

1 **Large mixing ratios of atmospheric nitrous acid (HONO) at Concordia (East Antarctic**  
2 **plateau) in summer: A strong source from surface snow?**

3  
4 Michel Legrand<sup>1,2</sup>, Susanne Preunkert<sup>1,2</sup>, Markus Frey<sup>3</sup>, Thorsten Bartels-Rausch<sup>4</sup>, Alexandre  
5 Kukui<sup>5,6</sup>, Martin D. King<sup>7</sup>, Joel Savarino<sup>1,2</sup>, Michael Kerbrat<sup>1,2</sup>, and Bruno Jourdain<sup>1,2</sup>

6  
7 <sup>1</sup> Univ. Grenoble Alpes, LGGE, F-38000 Grenoble, France

8 <sup>2</sup> CNRS, LGGE, F-38000 Grenoble, France

9 CNRS/Univ. Grenoble Alpes, Laboratoire de Glaciologie et Géophysique de l'Environnement  
10 (LGGE) UMR 5183, Grenoble, F-38041, France

11 <sup>3</sup> British Antarctic Survey (BAS), Natural Environment Research Council, Cambridge, UK

12 <sup>4</sup> Laboratory of Radio and Environmental Chemistry, Paul Scherrer Institute (PSI), 5232  
13 Villigen, Switzerland

14 <sup>5</sup> Laboratoire des Atmosphères, Milieux, Observations Spatiales (LATMOS), Paris, France

15 <sup>6</sup> Laboratoire de Physique et Chimie de l'Environnement et de l'Espace (LPC2E) UMR-  
16 CNRS, Orléans, France

17 <sup>7</sup> Department of Earth Sciences, Royal Holloway University of London, Egham, Surrey,  
18 TW20 0EX, UK

19  
20 Correspondence email: Legrand@lgge.obs.ujf-grenoble.fr

21  
22  
23  
24 **Abstract**

25 During the austral summer 2011/2012 atmospheric nitrous acid was investigated for the  
26 second time at the Concordia site (75°06'S, 123°33'E) located on the East Antarctic plateau  
27 by deploying a long path absorption photometer (LOPAP). Hourly mixing ratios of HONO  
28 measured in December 2011/January 2012 ( $35 \pm 5.0$  pptv) were similar to those measured in  
29 December 2010/January 2011 ( $30.4 \pm 3.5$  pptv). The large value of the HONO mixing ratio at  
30 the remote Concordia site suggests a local source of HONO in addition to weak production  
31 from oxidation of NO by the OH radical. Laboratory experiments demonstrate that surface  
32 snow removed from Concordia can produce gas phase HONO at mixing ratios half that of  
33 NO<sub>x</sub> mixing ratio produced in the same experiment at typical temperatures encountered at  
34 Concordia in summer. Using these lab data and the emission flux of NO<sub>x</sub> from snow

1 estimated from the vertical gradient of atmospheric concentrations measured during the  
2 campaign, a mean diurnal HONO snow emission ranging between  $0.5$  and  $0.8 \times 10^9$  molecules  
3  $\text{cm}^{-2} \text{s}^{-1}$  is calculated. Model calculations indicate that, in addition to around  $1.2$  pptv of  
4 HONO produced by the NO oxidation, these HONO snow emissions can only explain  $6.5$  to  
5  $10.5$  pptv of HONO in the atmosphere at Concordia. To explain the difference between  
6 observed and simulated HONO mixing ratios, tests were done both in the field and at lab to  
7 explore the possibility that the presence of  $\text{HNO}_4$  had biased the measurements of HONO.

## 9 **1. Introduction**

10 The existence of an oxidizing boundary layer over the Antarctic continent was first  
11 highlighted by measurements carried out at the South Pole, where a mean concentration of  
12  $2.5 \times 10^6$  OH radicals  $\text{cm}^{-3}$  was observed (Mauldin et al., 2001a), making the South Pole  
13 atmospheric boundary layer as oxidative as the remote tropical marine boundary layer  
14 (Mauldin et al., 2001b). Chen et al. (2001) and Davis et al. (2001) showed that the presence of  
15 high concentrations of  $\text{NO}_x$  produced by the photolysis of nitrate present in surface snow  
16 permits the required efficient recycling of  $\text{HO}_2$  into OH. Aside from snow photochemical  
17 emission of  $\text{NO}_x$  that acts as a secondary source of OH, the role of HONO as a primary source  
18 of OH remains unclear. Using a mist chamber followed by ion chromatography analysis of  
19 nitrite, Dibb et al. (2004) reported a median HONO mixing ratio close to  $30$  pptv at the South  
20 Pole. However, follow-up measurements by laser-induced fluorescence (LIF) indicated lower  
21 mixing ratios ( $6$  pptv on average) and an interference with  $\text{HNO}_4$  has been suspected (Liao et  
22 al., 2006). Furthermore, as discussed by Chen et al. (2004) the consideration of  $30$  pptv of  
23 HONO in the lower atmosphere over the South Pole leads to an OH over-prediction by gas-  
24 phase photochemical models by a factor of  $3$  to  $5$ . The authors questioned whether the  
25 discrepancy between observed and simulated concentrations of OH at the South Pole was due  
26 to measurements of HONO suffering from overestimation due to chemical interferences or if  
27 the mechanisms of the model missed  $\text{HO}_x$  and  $\text{NO}_x$  losses.

28 Even at the level of a few pptv, the presence of HONO requires a source other than the  
29 gas-phase reaction of NO with OH and many studies measuring HONO in atmospheres  
30 overlying snow covered regions suspected HONO to be emitted from the surface snow in  
31 addition to  $\text{NO}_x$  (see Grannas et al. (2007) for a review). It has to be emphasized that most of  
32 the studies of HONO have concerned high (Arctic, Greenland) and mid (Colorado and Alps)  
33 northern latitudes where, in relation to the chemical composition of snow, the involved  
34 HONO production processes would be very different compared to the case of Antarctica.

1 Concerning Antarctic snow, following the pioneering shading experiment done by Jones et al.  
2 (2000) on snow from the coastal Antarctic site of Neumayer, numerous studies investigated  
3 the release of NO<sub>x</sub> from the snow (see references in Frey et al., to be submitted), but only two  
4 studies reported on HONO snow emissions and none of them examined together HONO and  
5 NO<sub>x</sub> emissions. Beine et al. (2006) reported small HONO fluxes ( $3 \times 10^7$  molecule cm<sup>-2</sup> s<sup>-1</sup>)  
6 above the Browning Pass (coastal Antarctic) snowpack. However, the snow chemical  
7 composition at that site is very atypical with a large presence of calcium (up to 4 ppm)  
8 attributed to the presence of a lot of rock out-crops at the site. As a consequence, even if  
9 nitrate is abundant (typically 200 ppb in fresh snow and more than 1 ppm in aged snow), the  
10 snow from that site appears to be weakly acidic and sometimes alkaline. Finally a few  
11 investigations of the vertical distribution of HONO were made at the South Pole (Dibb et al.,  
12 2004) but no fluxes were calculated. These previous Antarctic studies of HONO were using  
13 either mist chambers (Dibb et al., 2002) or high-performance liquid chromatography  
14 techniques (Beine et al., 2006). These “wet chemical instruments” sample HONO on humid  
15 or aqueous surfaces followed by analysis of the nitrite ion. However, it is well known that  
16 many heterogeneous reactions lead to the formation of nitrite on similar surfaces (Gutzwiller  
17 et al., 2002, Liao et al., 2006). In addition to these chemical interferences, it is also known  
18 that HONO can decompose or be formed on various surfaces (Chan et al., 1976). That may  
19 affect data when sampling lines of up to 30 m length were used for polar measurements (see,  
20 e.g., Beine et al., 2006).

21 Motivated by a strong need to extend investigations of the oxidation capacity of the  
22 lower atmosphere at the scale of the whole Antarctic continent, the OPALE (Oxidant  
23 Production over Antarctic Land and its Export) project was initiated at the end of 2010 in East  
24 Antarctica. The first OPALE campaign was conducted during austral summer 2010/2011 at  
25 the coastal site of Dumont D’Urville (Preunkert et al., 2012) and focused on OH and RO<sub>2</sub>  
26 measurements (Kukui et al., 2012). During this first campaign, preliminary investigations of  
27 HONO were performed at the continental station of Concordia located at Dome C (denoted  
28 DC, 3233 m above sea level). In spite of the use of a long path absorption photometer  
29 (LOPAP), thought to avoid all known artefacts, high mixing ratios of HONO were observed  
30 (from 5 to 59 pptv, Kerbrat et al., 2012). In the framework of the OPALE project, a second  
31 summer campaign (2011-2012) was conducted at Concordia with simultaneous measurements  
32 of HONO, NO, NO<sub>2</sub>, OH and RO<sub>2</sub> that are discussed in a set of companion papers of which  
33 this is one.

1 The paper presented here focuses on HONO data gained during the second campaign at  
2 Cohnordia. It also reports on snow irradiation experiments conducted in the laboratory at  
3 British Antarctic Survey (BAS) on surface snow samples collected at DC in view to quantify  
4 a possible photochemical snow source of HONO. This was done by measuring  
5 simultaneously HONO with the LOPAP, NO and NO<sub>2</sub> with a 2-channel chemiluminescence  
6 detector. From these data we crudely estimate the amount of HONO released from snow  
7 within the lower atmosphere at DC on the basis of the NO<sub>x</sub> snow emissions derived from the  
8 vertical gradient of atmospheric concentrations measured during the campaign by Frey et al.  
9 (to be submitted). The derived values of the HONO flux were used in 1D modeling  
10 calculations to evaluate the contribution of this snow source to the large HONO mixing ratios  
11 observed at Cohnordia. Finally, to evaluate a suspected possible interference of HNO<sub>4</sub> on the  
12 HONO mixing ratio measured by the LOPAP, field experiments were conducted by heating  
13 sampled air prior to its introduction in the LOPAP device, heating being a convenient way to  
14 destroy HNO<sub>4</sub>. The selectivity to HNO<sub>4</sub> and the response of the LOPAP during the heating  
15 events was also investigated in laboratory by mass spectrometry at Paul Scherrer Institute  
16 (PSI).

17

## 18 **2. Methods and Site**

### 19 **2.1 HONO measurement method**

20 HONO was measured using a long path absorption photometer (LOPAP) which has  
21 been described in detail elsewhere (Heland et al., 2001; Kleffmann et al., 2002). In brief, after  
22 being sampled into a temperature controlled stripping coil containing a mixture of  
23 sulfanilamide in a 1N HCl solution, HONO is derivatized into a coloured azo dye. The light  
24 absorption by the azo dye is measured in a long path absorption tube by a spectrometer at 550  
25 nm using an optical path length of 5 m. The LOPAP did not have long sampling lines or inlet.  
26 The stripping coil was placed directly in the atmosphere being sampled. The LOPAP has two  
27 stripping coils connected in series to correct interferences. In the first coil (channel 1), HONO  
28 is trapped quantitatively together with a small amount of the interfering substances. Assuming  
29 that these interfering species are trapped in a similar amount in the second coil (channel 2),  
30 the difference between the signals resulting from stripping in each coil provides an  
31 interference-free HONO signal (Heland et al., 2001) Air was sampled at a flow rate of 1 L  
32 min<sup>-1</sup> and the flow rate of the stripping solution was of 0.17 mL min<sup>-1</sup>. Calibrations were  
33 performed every five days. Relative deviations of the calibration signal were of 3% and 9% at  
34 3σ for channel 1 and 2, respectively. The quantification limit of the LOPAP instrument used

1 in this study was as low as 1.5 pptv (taken as  $10 \sigma$  of all zero measurements done by sampling  
2 pure  $N_2$ ) with a time resolution of 9 min. More details on the set up of the LOPAP device in  
3 the fields can be found in Kerbrat et al. (2012). Similarly to the first campaign, the amount of  
4 interferences in the second coil was on average  $9 \pm 7 \%$  of total signal (instead of  $10 \pm 5 \%$   
5 found by Kerbrat et al. (2012) in 2010/2011). The LOPAP was tested for numerous possible  
6 interfering species including NO,  $NO_2$ ,  $HNO_3$ , and alkylnitrates. It was concluded that when  
7 significant the two channels approach was able to well correct the HONO data (Kleffmann  
8 and Wiesen, 2008). It has, however, to be emphasized that no tests have been conducted for  
9  $HNO_4$ .

10 During the field campaign, HONO was occasionally sampled in the snow interstitial air  
11 by pumping air through a PFA tube (5 m long, 4 mm internal diameter) at a flow rate of 1 L  
12  $min^{-1}$ . In addition, to evaluate a possible influence of  $HNO_4$  on HONO measurements, field  
13 experiments were undertaken by heating air sampled through a 9 m long PFA tube. Tests  
14 were performed to evaluate potential loss or formation of HONO in the PFA tubes by running  
15 the LOPAP for 30 min with and without a tube connected to the inlet of the LOPAP,  
16 sampling air at the same height. In order to account for possible fast natural change of HONO  
17 mixing ratios the test was repeated three times successively. The tests were carried out with  
18 ambient mixing ratios of 20 pptv as encountered at mid-day December 23<sup>rd</sup> and 40 pptv in the  
19 morning December 28<sup>th</sup>. In the two cases losses of around 4 pptv and 7 pptv were observed  
20 when using the 5 m and 9 m long PFA tube, respectively. These losses will be considered in  
21 discussing HONO mixing ratios in interstitial air (see Sect. 3) or the interference of  $HNO_4$   
22 (see Sect. 6).

23

## 24 **2.2 Field atmospheric measurements and snow samplings**

25 The second OPAL field campaign took place at Concordia located over the high East  
26 Antarctic plateau from late November 2011 to mid-January 2012. Nitrous acid was measured  
27 1 m above ground level, about 900 m south-southwest from the main Concordia station.  
28 Measurements that started December 4<sup>th</sup> were interrupted from December 9<sup>th</sup> to 15<sup>th</sup>,  
29 December 16<sup>th</sup> to 18<sup>th</sup>, and December 28<sup>th</sup> to 30<sup>th</sup> afternoon due to problems on the LOPAP  
30 device. January 1<sup>st</sup>, 2<sup>nd</sup>, and from January 10<sup>th</sup> to 13<sup>th</sup> air measurements were stopped to  
31 measure HONO in snow interstitial air. During the measurement campaign, the main wind  
32 direction was from the southeast to southwest. Several episodes with wind blowing from  
33 North (from  $10^\circ W$  to  $60^\circ E$  sector), i.e. from the direction of the station, were encountered  
34 (see the red points in Fig. 1). During some of these pollution events (December 31<sup>st</sup> around

1 22:00 for instance), sharp peaks of HONO mixing ratios exceeding 100 pptv were observed.  
2 These events were also detected in the NO<sub>x</sub> time series (Frey et al., to be submitted) with  
3 sharp peaks in the range of 100 ppbv or more (120 ppbv December 31<sup>st</sup> around 22:00 for  
4 instance). The ratio of excess of HONO to excess of NO<sub>x</sub> during these events is close to 10<sup>-3</sup>.  
5 The ratios of HONO/NO<sub>x</sub> reported by measurements made in traffic tunnels range from 3x10<sup>-3</sup>  
6 (Kirchstetter et al., 1996) to 8x10<sup>-3</sup> (Kurtenbach et al., 2001). When compared to ratios  
7 observed in tunnels, the lower ratio seen in the plume of the Concordia station when it reaches  
8 the sampling line is likely due the rapid photolytic destruction of HONO whose the lifetime is  
9 still as short as 20 min at the high solar zenith angles prevailing at DC around 22:00 in  
10 summer. In the following the data corresponding to red points reported in Fig. 1 were  
11 removed from the HONO data set.

12 Concurrent measurements of chemical species that are relevant for discussion include  
13 ozone, NO, NO<sub>2</sub>, OH, and RO<sub>2</sub>. Surface ozone was monitored simultaneously to HONO using  
14 UV absorption monitors (Thermo electron Corporation model 49I) deployed at Concordia  
15 since 2007 (Legrand et al., 2009). Nitrogen oxides were determined by deploying a 2-channel  
16 chemiluminescence detector (Bauguitte et al., 2012; Frey et al., 2013; Frey et al., to be  
17 submitted). The chemiluminescence detector measured NO in one channel and the sum of  
18 NO, and NO originating from the photolytic conversion of NO<sub>2</sub> in the other channel. As  
19 discussed by Frey et al. (2013), among various nitrogen oxides able to interfere on the  
20 photolytic conversion channel only HONO has to be considered leading to an overestimation  
21 of NO<sub>2</sub> levels by less than 5%. The radicals (OH and RO<sub>2</sub>) were measured using chemical  
22 ionisation mass spectrometry (Kukui et al., 2012; Kukui et al., 2014). During the campaign  
23 the photolysis rate of HONO was documented using a Met-Con 2π spectral radiometer  
24 equipped with a CCD detector and a spectral range from 285 to 700 nm (see details in Kukui  
25 et al., 2014).

26 Different surface snow samples were collected at DC and returned to the UK to be used  
27 in irradiation experiments (see Sect. 2.3 and Sect. 4). First, the upper 12 cm of snow were  
28 collected in December 2010. Second, the upper centimetre of snow corresponding to freshly  
29 drifted snow was collected December 6<sup>th</sup> 2011. The samples were characterized by their  
30 specific surface area (SSA). Measurements were performed using an Alpine Snowpack  
31 Specific Surface Area Profiler, an instrument similar to that one described by Arnaud et al.  
32 (2011) based on the infrared reflectance technique. Briefly, a laser diode at 1310 nm  
33 illuminates the snow sample at nadir incidence angle and the reflected hemispherical radiance  
34 is measured. The hemispherical reflectance at 1310 nm is related to the SSA using the

1 analytical relationship proposed by Khokanovsky and Zege (2004). The SSA of the drifting  
2 snow is close to  $26 \text{ m}^2 \text{ kg}^{-1}$ , and the upper 12 cm is  $17 \text{ m}^2 \text{ kg}^{-1}$ . Such values appear to be close  
3 to typical DC values reported in the literature (Gallet et al., 2011), suggesting that lab  
4 experiments conducted on these snow samples (see Sect. 4) may be relevant to discuss at least  
5 qualitatively natural processes occurring at DC.

6 The upper surface snow (from 0 to 1 cm, and from 0 to 12 cm) at DC were also sampled  
7 and analysed for major anions and cations following working conditions reported in Legrand  
8 et al. (2013). For cations ( $\text{Na}^+$ ,  $\text{K}^+$ ,  $\text{Mg}^{2+}$ ,  $\text{Ca}^{2+}$ , and  $\text{NH}_4^+$ ), a Dionex 500 chromatograph  
9 equipped with a CS12 separator column was used. For anions, a Dionex 600 equipped with an  
10 AS11 separator column was run with a quaternary gradient of eluents ( $\text{H}_2\text{O}$ ,  $\text{NaOH}$  at 2.5 and  
11 100 mM, and  $\text{CH}_3\text{OH}$ ) allowing the determination of inorganic species ( $\text{Cl}^-$ ,  $\text{NO}_3^-$ , and  $\text{SO}_4^{2-}$ )  
12 as well as methanesulfonate ( $\text{CH}_3\text{SO}_3^-$ ). The acidity of samples can be evaluated by the ionic  
13 balance between anions and cations with concentrations expressed in micro-equivalents per  
14 liter ( $\mu\text{Eq L}^{-1}$ ):

$$15 \quad [\text{H}^+] = [\text{Cl}^-] + [\text{NO}_3^-] + [\text{SO}_4^{2-}] + [\text{CH}_3\text{SO}_3^-] - [\text{Na}^+] - [\text{K}^+] - [\text{Mg}^{2+}] - [\text{Ca}^{2+}] - [\text{NH}_4^+] \quad (1)$$

16

### 17 **2.3 Snow irradiation experiments conducted at BAS**

18 As discussed in Sect. 5, model simulations indicate that the production of HONO from  
19 the reaction of OH with NO is far too weak to explain observations at Concordia and that an  
20 additional light driven HONO source is needed. To quantify a possible photochemical snow  
21 source of HONO, lab experiments were conducted at BAS by irradiating snow collected at  
22 DC and measuring gas-phase evolution of NO and  $\text{NO}_2$  with a 2-channel chemiluminescence  
23 detector (Bauguitte et al., 2012) as deployed at Concordia (Frey et al. 2013, Frey et al. to be  
24 submitted) and HONO with the LOPAP that ran at to Concordia during the 2010/2011 and  
25 2011/2012 campaigns. A 20 cm long cylinder (6 cm inner diameter) was filled with  $\sim 120 \text{ g}$   
26 of snow inside an airtight glass reaction chamber (total length of 40 cm, 6 cm inner diameter)  
27 and put in a freezer of which the temperature was varied between  $-5$  to  $-35^\circ\text{C}$ . Further details  
28 on the characteristics of the reaction chamber can be found in Meusinger et al. (2014). The  
29 reaction chamber is maintained vertically in a freezer and a 1000 W Xenon-arc lamp was put  
30 above the freezer. The snow was irradiated by directing the light axially along the tube  
31 through a quartz window, which makes up the top surface of the chamber. Chemically pure  
32 air was supplied to the chamber from a pure air generator (Ecophysics, PAG003) in which air  
33 is dried at  $-15^\circ\text{C}$ . To match the relative humidity of the snow under investigation and limit  
34 metamorphism the chemically pure (humid) air dry was passed through a cold trap at the

1 temperature of the experiment. Note that with this system and for temperatures above  $-30^{\circ}\text{C}$ ,  
2 no condensation trace was observed in the tubes outflow of the chamber. The flow rate of  
3 zero air was  $4.3\text{ L min}^{-1}$  while the detection systems sampled processed air at a rate of  $2.0\text{ L}$   
4  $\text{min}^{-1}$  for  $\text{NO}_x$  and  $1.0\text{ L min}^{-1}$  for HONO. The overflow of  $1.3\text{ L min}^{-1}$  was diverted through a  
5 flow metre to check for potential leaks. While the inlet line between the reaction chamber and  
6 the  $\text{NO}_x$  analyser was several m long, the length between the outlet of the reaction chamber  
7 and the LOPAP inlet was kept as short as possible (i.e. 25 cm). To do so the inlet of the  
8 LOPAP was arranged in the freezer. The wavelength range of the 1000 W Xenon-arc lamp  
9 (Oriel Instruments) was 200-2500 nm, modulated using filters with various cut-on points. The  
10 short residence time of  $\text{NO}_2$  ( $\sim 4\text{ s}$ ) in our small chamber prevents significant photolysis of  
11  $\text{NO}_2$  to occur during the experiments. Indeed, the  $J_{\text{NO}_2}$  of  $2\text{ }10^{-2}\text{ s}^{-1}$  measured by Cotter et al.  
12 (2003) for a 1000 W Xenon-arc lamp, as also used in the present study, leads to a lifetime of  
13  $\text{NO}_2$  with respect to photolysis of 50 s at the front of the snow block.

14

#### 15 **2.4 Experiments performed at PSI to investigate a possible $\text{HNO}_4$ interference on** 16 **HONO measurements**

17 As will be discussed in Sect. 6, it may be difficult to reconcile typical mixing ratios of  
18 HONO measured 1 m above surface snow at Concordia with a reasonable estimate of the  
19 mixing ratio of HONO owing to emissions from snow due to snowpack photochemistry. It  
20 was suspected that  $\text{HNO}_4$  was detected and measured as HONO by the LOPAP instrument.  
21 As briefly reported below, a few experiments conducted at PSI indicate that the LOPAP  
22 instrument does have an interference for  $\text{HNO}_4$ . Mixing ratios of  $\text{HNO}_4$  were not measured at  
23 Concordia, so the aim of the experiments described below was not to quantify the interference  
24 to enable correction of the Concordia HONO data, but to demonstrate that such an  
25 interference exists. The result of an experiment conducted under specific conditions is  
26 reported. A full characterization of the interference on HONO at various mixing ratios of  
27  $\text{HNO}_4$  in the presence or not of other trace gases present at DC is beyond the scope of this  
28 paper.

29 The interference of the LOPAP device was examined at the PSI where a gas-phase  
30 synthesis of  $\text{HNO}_4$  has been developed by irradiating a mixture of  $\text{NO}_2/\text{H}_2\text{O}/\text{CO}/\text{O}_2/\text{N}_2$  at 172  
31 nm (Bartels-Rausch et al., 2011). By-products of the synthesis are HONO,  $\text{HNO}_3$ , and  $\text{H}_2\text{O}_2$ .  
32 The synthesis gas was fed into the sampling unit of the LOPAP and the resulting LOPAP  
33 signals in presence and absence of  $\text{HNO}_4$  were compared. Heating the synthesis gas to a  
34 temperature of  $100^{\circ}\text{C}$  prior to sampling by the LOPAP allowed selective removal of  $\text{HNO}_4$



1 from the gas mixture. The mixing ratios of HONO, NO<sub>2</sub>, H<sub>2</sub>O<sub>2</sub> and O<sub>3</sub> that are present in the  
2 synthesis gas were independently monitored with a chemical ionisation mass spectrometer  
3 (CIMS), which was calibrated by using several analysers as detailed in Ulrich et al. (2012).  
4 An example of the mixing ratios of HNO<sub>4</sub> and HONO measured by CIMS and of the  
5 corresponding LOPAP signals in channel 1 and 2 is shown in Fig. 2. The relative amount of  
6 HONO (780 pptv) and HNO<sub>4</sub> (1000 pptv) observed in the synthesized mixture (prior heating)  
7 is typical for this synthesis (Bartels-Rausch et al., 2011). The experiment shows the response  
8 of the signals when the heating trap used to decompose HNO<sub>4</sub> is applied. As seen in Fig. 2,  
9 the mixing ratios of HONO, NO<sub>2</sub>, H<sub>2</sub>O<sub>2</sub> or O<sub>3</sub> that may influence the response of the LOPAP  
10 instrument did not change upon the thermal decomposition of HNO<sub>4</sub>. A decrease of the  
11 LOPAP signal in channel 1 is observed during the heating event, indicating that 1 ppbv of  
12 HNO<sub>4</sub> corresponds to a signal in the LOPAP of 150 pptv. Examination of the signals of the  
13 two LOPAP channels (Fig. 2) suggests that HNO<sub>4</sub> has been efficiently sampled in the first  
14 channel. It is well known that HNO<sub>4</sub> efficiently decomposes to NO<sub>2</sub><sup>-</sup> in acidic solutions  
15 (Regimbal and Mozurkewich, 1997), just like HONO does in the LOPAP sample unit. Based  
16 on the identical hydrolysis products, one might thus expect a rather large interference. The  
17 high sampling efficiency of HONO and potentially HNO<sub>4</sub>, both of which have similar  
18 partitioning coefficients to acidic solutions, is driven by the fast reaction of their hydrolysis  
19 product (NO<sub>2</sub><sup>-</sup>) with the reagents in the sampling solution of the LOPAP instrument. A full  
20 characterization of the interference by HNO<sub>4</sub> (its behaviour and quantification over a large  
21 range of concentrations, in the presence or absence of other gases) is needed to improve the  
22 use of the LOPAP in very cold atmospheres. We suggest a detailed investigation of LOPAP  
23 instrument response to different compositions of test gas mixture (i.e. with larger mixing  
24 ratios of H<sub>2</sub>O<sub>2</sub>), and with an investigation of the potentially complex (non-linear) chemistry of  
25 sampled gases. At this stage we can only exclude an oxidation of the dye used in the LOPAP  
26 instrument by HNO<sub>4</sub>, as careful inspection of the absorption spectrum of the LOPAP dye  
27 reveals no significant change during heating. Assuming the interference of HONO signal by  
28 HNO<sub>4</sub> to be linear, one would expect an interference of ~15 pptv in the HONO signal due to a  
29 mixing ratio of 100 pptv of HNO<sub>4</sub>. Given the absence of measurements of the mixing ratio of  
30 HNO<sub>4</sub> at Concordia, further experiments were conducted in the field at Concordia to directly  
31 estimate this interference as detailed in Sect. 6.

32

### 33 **3. HONO observations at Concordia**

1 Removing data suspected to have been impacted by pollution from station activities (see  
2 Sect. 2.2), one-minute average mixing ratio of  $35 \pm 14$  pptv is observed in December  
3 2011/January 2012 compared to  $28 \pm 12$  pptv measured by Kerbrat et al. (2012) for December  
4 2010/ January 2011.

5 The mean diurnal cycles of surface ozone, HONO, air temperature and the PBL height  
6 simulated by the regional atmospheric MAR model (Modèle Atmosphérique Régional) are  
7 reported and compared for the two summers in Fig. 3. In polar region, the strong static  
8 stability of the atmosphere often inhibits vertical mixing of surface emissions between the  
9 surface boundary layer and the rest of the atmosphere. At DC, the surface absorbs solar  
10 radiations during the day, heats the lower atmosphere and generates positive buoyancy that is  
11 responsible for an increase of turbulent kinetic energy and the subsequent increase of the  
12 boundary layer height seen in Fig. 3. This boundary layer is referred to as the "daytime  
13 boundary layer". The surface cooling after 17:00 generates negative buoyancy near the  
14 surface. A new boundary layer referred as the "night-time boundary layer" develops but  
15 remains less active than the previous daytime boundary layer. The collapse of the boundary  
16 layer after 17:00 seen in Fig. 3 is in fact the representation of the transition between the  
17 daytime and nighttime boundary layer.

18 The two mean summer ozone records indicate a drop of 1 to 2 ppbv around mid-day  
19 compared to early morning and evening values (Fig. 3). This small surface ozone change over  
20 the course of the day at DC has already been observed by Legrand et al. (2009) who attributed  
21 it to the increase of the PBL height in the afternoon that counteracts a local photochemical  
22 production of  $O_3$  in the range of  $0.2$  ppbv  $hr^{-1}$  during day-time.

23 Consistently with the previous 2010/2011 measurements from Kerbrat et al. (2012), the  
24 HONO mixing ratios exhibit a well-marked diurnal variation characterized by morning  
25 (around 5:00-7:00) and evening (around 20:00) maxima exceeding mid-day values by some  
26 10 pptv. Therefore, in addition to an expected more efficient photolysis of HONO during the  
27 day, the increase of the daytime boundary layer may also accounts for the observed decreased  
28 HONO mixing ratios during the day in spite of a more active snow source (see discussions in  
29 Sect. 5). Such a diurnal variability characterized by noon minimum was also observed for  
30  $NO_x$  by Frey et al. (2013) and attributed to the interplay between photochemical snow source  
31 and boundary layer dynamics.

32 As shown in Fig. 3, the larger HONO mixing ratios calculated for 2011/2012 (diurnal  
33 mean of  $35 \pm 5.0$  pptv) with respect to the 2010/2011 ones (diurnal mean of  $30.5 \pm 3.5$  pptv)  
34 concern both the mid-day minimum and the morning/evening maxima. The difference

1 between the two summers is however reduced when the first week of measurements  
2 undertaken December in 2011 is removed with a lower diurnal mean ( $31.7 \pm 4.3$  pptv instead  
3 of  $35 \pm 5$  pptv over the entire measurement period, see the blue points in Fig. 3). The case of  
4 beginning of December 2011 with respect to the rest of the summer 2011/2012 is highlighted  
5 in Fig. 3. It can be seen that the far thinner PBL height of early December (maximum of 145  
6 m instead of 350 m over the entire period) may have lead to a more confined HONO  
7 production (see violet points in Fig. 3). Note also the relatively high ozone mixing ratios at  
8 that time ( $33 \pm 4$  ppbv in early December instead of  $26 \pm 1$  ppbv over the entire period).  
9 Conversely, at the end of the period the PBL became thicker (maximum of 570 m) and the  
10 mixing ratios of ozone ( $24 \pm 1$  ppbv) and nitrous acid ( $31 \pm 4$  pptv) were lower than on  
11 average (see red points in Fig. 3). Finally, early December 2011 the highest daily average  
12 mixing ratio of HONO observed December 7<sup>th</sup> and 8<sup>th</sup> (56 pptv, Fig. 1), correspond not only  
13 to a thin PBL but also to lowest value of total ozone column (260 Dobson Units (DU) instead  
14 of  $296 \pm 20$  DU on average) measured by the SAOZ at Concordia. Similarly, during the  
15 2010/2011 campaign the highest values reported at the end of the campaign (44 pptv from  
16 15<sup>th</sup> to 18<sup>th</sup> January) by Kerbrat et al. (2012) correspond to the lowest value of total ozone  
17 column (270 DU instead of  $303 \pm 17$  DU on average). It therefore seems that HONO mixing  
18 ratios measured at 1 m at DC are also sensitive to the UV actinic flux reaching the surface.  
19 This link between stratospheric ozone and photochemistry of snow at the ground is discussed  
20 in more detail by Frey et al. (to be submitted).

21 It therefore seems that one of the main causes for the difference between the 2011/2012  
22 and 2010/2011 mean summer values is the slightly different atmospheric vertical stability  
23 conditions experienced over the different sampling times of the two summers, with an earlier  
24 HONO sampling in December 2011 than in December 2010 leading to higher HONO mixing  
25 ratios in a very thin and stable boundary layer. In conclusion, this second study of HONO  
26 confirms the abundance of this species in the lower atmosphere at DC with a typical mean  
27 mixing ratio of 30 pptv from mid-December to mid-January.

28 As already discussed by Kerbrat et al. (2012) (see also Sect. 5), the existence of a large  
29 photochemical source of HONO in the snow-pack is needed to explain these large mixing  
30 ratios of HONO measured above the snowpack. Measurements of the mixing ratio of HONO  
31 were therefore performed in snow interstitial air at different depths. From the top few cm of  
32 the snowpack down to 75 cm depth, mixing ratios of HONO in snowpack interstitial air  
33 tended to exceed those in the air above the snowpack, supporting the existence of a snow  
34 source of HONO (Fig. 4). However, given the interference of  $\text{HNO}_4$  on HONO mixing ratio

1 data as discussed in Sect. 6, it is difficult to use the observed vertical gradient of HONO  
2 mixing ratio to derive an estimate of emission of HONO from the snowpack. Indeed, typical  
3 values of HNO<sub>4</sub> mixing ratios are available in lower atmosphere of the Antarctic plateau  
4 (Sect. 6) but not yet in snow interstitial air. Also it remains difficult to accurately estimate the  
5 production rate of HNO<sub>4</sub> in snow interstitial air from the reaction of NO<sub>2</sub> with HO<sub>2</sub> versus its  
6 uptake on natural ice surface.

7 To confirm the snowpack as a source of HONO (and as detailed in the following  
8 section) we carried out a laboratory experiment to evaluate the ratio of HONO to NO<sub>x</sub>  
9 released from natural surface snows collected at DC under controlled laboratory conditions  
10 (i.e. wavelength of light, temperature, snow specific area) to estimate the HONO snow  
11 emission flux relative to the snow emission flux of NO<sub>x</sub> for the same snowpack as derived  
12 from atmospheric concentration vertical gradient measured during the campaign by Frey et al.  
13 (to be submitted).

14

#### 15 **4. Lab experiments on natural snow collected at DC**

16 Table 1 summarized the results of experiments conducted at BAS by irradiating surface  
17 snows collected at DC (see Sect. 2.3). NO<sub>x</sub> and HONO are produced when snow is irradiated.  
18 Several laboratory experiments were conducted to investigate the wavelength, temperature  
19 and snow chemical composition dependence of HONO release from snow. Similar to  
20 previous laboratory experiments conducted by Cotter et al. (2003) on surface snows collected  
21 in coastal Antarctica, the NO<sub>x</sub> release is found to halve when the optical filter in the front of  
22 the irradiation lamp (cut off for < 295 nm) is replaced by a cut off filter for illumination  
23 wavelength smaller than 320 nm (Table 1). Cotter et al. (2003) demonstrated no measurable  
24 emission of NO<sub>x</sub> from the snow when illuminated with a lamp with wavelengths shaded  
25 below 345 nm, being consistent with NO<sub>3</sub><sup>-</sup> photolysis. Fig. 5 illustrates the wavelength  
26 dependence of HONO release showing the effect of insertion of a filter with different cut-on  
27 points. Similarly to the NO<sub>x</sub>, the HONO release is decreased by a factor two when inserting  
28 the filter at 320 nm and becomes insignificant at 385 nm (Table 1).

29 While the observed wavelength dependency of the NO<sub>x</sub> release supports the hypothesis  
30 that the photolysis of nitrate present in snow is the major source of released NO<sub>x</sub> (via its  
31 major channel: NO<sub>3</sub><sup>-</sup> + hv → NO<sub>2</sub> + O<sup>•</sup>), for HONO it is still unclear if either the nitrate  
32 photolysis efficiently produces directly HONO from hydrolysis of NO<sub>2</sub><sup>-</sup> produced by the  
33 second channel of the nitrate photolysis (NO<sub>3</sub><sup>-</sup> + hv → NO<sub>2</sub><sup>-</sup> + O), or HONO is secondarily  
34 produced from NO<sub>2</sub> (Villena et al., 2011). Indeed, lab experiments conducted on nitrate doped

1 ice suggest that the first channel is a factor of 8-9 more efficient than the second one. It is  
2 suspected that the HONO production may be significantly higher than it is when considering  
3 this second channel since the NO<sub>2</sub> produced by the first channel may subsequently act as a  
4 precursor of HONO. The wavelength dependency of HONO release observed during previous  
5 experiments does not however help to separate the primary and secondary source of HONO  
6 during irradiation since they were done with chemically pure air and when placing the cut off  
7 filter at 385 nm we suppress the primary source of HONO as well as NO<sub>2</sub> that is needed for  
8 secondary HONO production.

9       Among possible secondary productions it is generally accepted that the reduction of  
10 NO<sub>2</sub> on photo-sensitized organic material like humic acid (George et al., 2005; Bartels-  
11 Rausch et al., 2010) would proceed more efficiently than the disproportionation reaction of  
12 NO<sub>2</sub> ( $2 \text{ NO}_2 + \text{H}_2\text{O} \rightarrow \text{HONO} + \text{HNO}_3$ ) (Finlayson-Pitts et al., 2003). As discussed by  
13 Grannas et al. (2007), the relevance of this secondary production was supported even for  
14 Antarctica by the significant presence of dissolved fulvic acid reported for Antarctic snow  
15 (26-46 ppbC) by Calace et al. (2005). However, the previously assumed ubiquitous presence  
16 of organics in polar snow that is needed to reduce NO<sub>2</sub> into HONO was recently reviewed by  
17 Legrand et al. (2013) who found that organics (and humic acids) are far less abundant in  
18 Antarctica compared to Greenland or mid-latitude glaciers like the Alps. For instance, the  
19 typical dissolved organic content of summer surface snow is only 10-27 ppbC at DC (Legrand  
20 et al., 2013) against  $110 \pm 45$  ppbC at Summit and 300 ppbC in the Alps. Furthermore, recent  
21 HULIS measurements of surface snows collected at DC do not confirm the previously  
22 observed abundance (2 ppbC instead of 26-46 ppbC). From lab experiments conducted by  
23 irradiating ice films containing humic acid in the presence of NO<sub>2</sub>, Bartels-Rausch et al.  
24 (2010) derived production rates of HONO from NO<sub>2</sub>. From that the authors roughly estimated  
25 light driven HONO fluxes of  $10^{13}$  molecule m<sup>-2</sup> s<sup>-1</sup> from snow covered surface area assuming  
26 the presence of 100 pptv NO<sub>2</sub> in the snow interstitial air and a concentration of 10 ppbC of  
27 humic acid in snow. Keeping in mind uncertainties in extrapolating lab experiments to  
28 conditions relevant to the lower atmosphere at DC, with typical NO<sub>2</sub> mixing ratios of 1 to 10  
29 ppbv in interstitial air at 10 cm below the surface at DC (Frey et al., to be submitted), the  
30 presence of 2 ppbC of HULIS in snow may still lead to a significant HONO production from  
31 NO<sub>2</sub> at the site. If HULIS are located at the surface of snow grains, much more than 2 ppbC  
32 of HULIS would be available to react with NO<sub>2</sub> present in interstitial air of the snowpack to  
33 produce HONO.

34       Irradiation experiments with insertion of the filter at 295 nm were conducted at

1 temperatures ranging from 240 to 260 K. As seen in Table 1, whereas the NO<sub>x</sub> release was  
2 found to be temperature independent (as previously shown by Cotter et al., 2003), a large  
3 dependence is found for HONO with an increase by a factor of 2.2 when the temperature of  
4 snow is increased from 240 to 260 K. A temperature dependence of the HONO emissions is  
5 expected since the partition coefficient of HONO between ice and air increases by a factor of  
6 5.8 between 240 K and 260 K (Crowley et al., 2010). As a consequence the HONO to NO<sub>x</sub>  
7 release is smaller at 240K than at 260K. For the example of the surface snow reported in  
8 Table 1, this ratio steadily increases from 0.3 at 240 K, 0.5 at 250 K to 0.8 at 260 K.

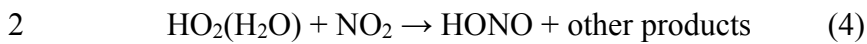
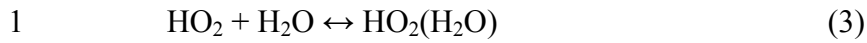
9 In Table 1 we report experiments with DC snow containing 160 to 1400 ppb of nitrate.  
10 As expected higher nitrate content leads to higher snow release of NO<sub>x</sub> and HONO but the  
11 increase of HONO is larger than NO<sub>x</sub>. For instance, at a temperature close to -20°C, the first  
12 upper cm of surface snow releases almost twice more HONO compared NO<sub>x</sub> than the snow  
13 collected from the surface to 12 cm depth. The more acidic character of the snow collected in  
14 the upper first centimetre compared to the one collected down to 12 cm below the surface (see  
15 Table 1) may favour the release of a weak acid species like HONO.

## 16 17 **5. Model calculations**

18  
19 Observed atmospheric mixing ratios were compared with steady-state calculations  
20 made by considering major gas-phase sources and sinks of HONO. The major sink of HONO  
21 is its photolysis. The photolysis rate constant ( $J_{\text{HONO}}$ ) were measured with a  $2\pi$   
22 spectroradiometer (see Sect. 2.2). The value of  $J_{\text{HONO}}$  was calculated for light from  $4\pi$   
23 steradians from the downwelling value of  $J_{\text{HONO}}$  measured over  $2\pi$  steradians by assuming a  
24 surface albedo of 0.95, a typical value for regions covered by dry snow and wavelength  
25 shorter than 400 nm (Hudson et al., 2006; France et al., 2011). The main gas-phase  
26 production of HONO is the reaction of NO with OH radicals. Steady-state calculations  
27 indicate that under noon conditions encountered at DC (a  $J_{\text{HONO}}$  value of  $3.7 \times 10^{-3} \text{ s}^{-1}$ ,  $5 \times 10^6$   
28 OH rad.  $\text{cm}^{-3}$  (Kukui et al., 2014), and 50 pptv of NO (Frey et al., to be submitted)), a HONO  
29 mixing ratio of 1 pptv is expected. Steady-state calculated diurnal HONO profile (Fig. 6)  
30 suggests a HONO maximum of 2.5 pptv at 19:00 due to the presence of a maximum of 120  
31 pptv of NO (Frey et al., to be submitted).

32 Another gas-phase source of HONO was recently proposed by Li et al. (2014) via  
33 reaction of the HO<sub>2</sub>(H<sub>2</sub>O) complex with NO<sub>2</sub>:





3

4 Reaction of the  $\text{HO}_2(\text{H}_2\text{O})$  complex with  $\text{NO}_2$  was first suggested by Sander and  
5 Peterson (1984) to explain the observation of a linear dependence of the effective rate  
6 constant of the reaction of  $\text{HO}_2$  with  $\text{NO}_2$  on the concentration of water vapour in the  
7 temperature range 275-298 K. Assuming reaction mechanism (2-4) Sander and Peterson  
8 (1984) derived temperature dependence for the effective third-order rate constant of the  
9 reaction  $\text{HO}_2 + \text{NO}_2 + \text{H}_2\text{O}$ ,  $k^{\text{III}}_4(\text{T})$ , with  $k^{\text{III}}_4(\text{T})$  representing the product  $k_4 \times K_3$ , where  $k_4$  is the  
10 bimolecular rate constant for reaction  $\text{HO}_2(\text{H}_2\text{O})$  with  $\text{NO}_2$  and  $K_3$  is equilibrium constant for  
11 reaction (3). The possible contribution of reaction (4) to form HONO at Concordia was  
12 evaluated by assuming a unity yield of HONO for the reaction (4). The rate constant  $k_4(\text{T})$  in  
13 the temperature range 275-298 K was estimated from the  $k^{\text{III}}_4(\text{T})$  data of Sander and Peterson  
14 (1984) using recent recommendations for  $K_3(\text{T})$  and  $k_2(\text{T})$  from Sander et al. (2011):  $k_4(\text{T}) =$   
15  $k^{\text{III}}_4(\text{T}) / K_3(\text{T}) \times k_2(\text{T}) / k_2(\text{T})^{\text{Sander}}$ , where  $k_2(\text{T})^{\text{Sander}}$  are data from Sander and Peterson  
16 (1984). The values of  $k_4(\text{T})$  at low temperatures encountered at Concordia were obtained by  
17 extrapolating the  $k_4(\text{T})/k_2(\text{T})$  data from Sander and Peterson (1984) and assuming a  
18 logarithmic dependence of  $k_4(\text{T})/k_2(\text{T})$  on  $1/\text{T}$ , similar to reaction of  $\text{HO}_2(\text{H}_2\text{O})$  with  $\text{HO}_2$   
19 (Sanders et al., 2011). The resulting dependence ( $k_4(\text{T})/k_2(\text{T}) = 10^{-1505.3/\text{T}(\text{K})+5.4}$ ) predicts  
20 significantly lower water enhancement effect at low temperature ( $k_4/k_2=0.12$  at 240K  
21 compared to 2.2 at 298K). Using these  $k_4$  values and observations of OH, NO,  $\text{HO}_2$ ,  $\text{NO}_2$  and  
22  $\text{H}_2\text{O}$ , the low temperatures encountered at Concordia render the formation of HONO from the  
23 reaction (4) negligible. This hypothetical HONO source would contribute for 10-20% of the  
24 HONO production from the reaction  $\text{OH} + \text{NO}$  and would result in less than 1% of the  
25 measured HONO.

26 An additional source of HONO is obviously required to account for observed mixing  
27 ratios of a few tens of pptv. On the basis of laboratory experiments presented in Sect. 4, we  
28 examine to what extent the snow photochemical source of HONO accounts for atmospheric  
29 observations of HONO at Concordia. Simulations were made with a numerical 1-D box  
30 model that considers, in addition to the above-mentioned gas-phase sources and sinks of  
31 HONO, a flux from the snow and its diffusive vertical transport. The turbulent diffusion  
32 coefficients ( $K_z$ ) were calculated by the regional atmospheric MAR model. Since cloud cover  
33 is responsible for an increase of around 50% of the down-welling long-wave radiations in  
34 summer at DC, when the cloud cover is underestimated, the surface heat budget is not well

1 simulated and this strongly impacts the turbulence simulated by the model. We therefore  
2 performed calculations only for days with clear sky conditions (see Fig. 1).

3 We used the MAR model with a horizontal resolution of 20 km centred at Concordia;  
4 a top level is at 1 hPa with 100 vertical levels. The vertical resolution is 0.9 m up to 23 m  
5 above the surface, and decreases upward. MAR  $K_z$  values are linearly interpolated to the  
6 vertical grid used in our 1D simulation, spacing 0.1 m from the ground to 5 m, 0.2 m from 5  
7 to 7 m, 0.5 m from 7 to 10 m, around 1 m from 10 to 20 m and then increases up to 120 m at  
8 1200 m height, respectively. MAR data above a height of 1200 m were not used here since  
9 during investigated period the top of the PBL remained below this value. The MAR model  
10 uses primitive equations with the hydrostatic assumption. A description of the model that has  
11 been validated with respect to observations from Automatic Weather Station at Concordia, is  
12 given by *Gallée and Gorodetskaya* [2008] and references therein. Parametrization of  
13 turbulence in the lowest model layer of MAR is based on the Monin-Obukhov Similarity  
14 theory (MOST). Above the surface boundary layer, turbulence is parametrized using the E -  $\epsilon$   
15 model that includes two prognostic equations for turbulent kinetic energy and its dissipation.  
16 MAR simulations have been recently validated with respect to observations from the  
17 Automatic Weather Station at Concordia for winter (*Gallée and Gorodetskaya*, 2008) and  
18 summer (*Gallée et al.*, to be submitted). The boundary layer (PBL) height was computed from  
19 MAR simulations by taking the height where the turbulent kinetic energy decreases below 5  
20 % of the value of the lowest layer of the model.

21 In Fig. 6 we report the simulated diurnal cycle of HONO mixing ratio at 1 m above the  
22 ground at Concordia when a photochemical snow release of HONO is applied. The HONO  
23 flux used in these calculations was obtained by multiplying the values of the  $\text{NO}_x$  snow  
24 emission flux derived from field observations at Concordia (*Frey et al.*, to be submitted) by  
25 the temperature dependent factor reported for surface snow in Table 1. Since, as discussed in  
26 section 4, lab experiments indicate no significant change of the ratio of HONO/ $\text{NO}_x$  release  
27 when replacing the filter with a 295 nm cut-off point by the one at 320 nm (Table 1), and  
28 given a maximum of the aqueous absorption cross section for nitrate centered at 300 nm  
29 (*Gaffney et al.*, 1992), we have assumed that the ratio is similar under the two wavelength  
30 conditions and used the temperature dependency found when the filter with a cut-off point at  
31 295 nm was inserted (Table 1). In this way under temperature conditions encountered at DC  
32 we have assumed a HONO/ $\text{NO}_x$  ratio ranging from 0.57 during the day (at  $-25^\circ\text{C}$ ) and 0.3 at  
33 night (at  $-35^\circ\text{C}$ ). The derived HONO snow emission flux estimate would represent an upper  
34 limit since, as seen in Sect. 4, the upper 12 cm of snow emits less HONO than  $\text{NO}_x$  compared



1 to the surface snow. As seen in Fig. 6, using this upper estimate of the HONO snow emission  
2 (mean diurnal value of  $0.8 \times 10^9$  molecules  $\text{cm}^{-2} \text{s}^{-1}$ ) simulations show that, in addition to  
3 around 1.2 pptv of HONO produced by the NO oxidation, the HONO snow emissions can  
4 account for 10.5 pptv of HONO in the atmosphere at Concordia. Assuming a lower HONO to  
5  $\text{NO}_x$  ratio of snow emissions as suggested by the experiment conducted with the upper 12 cm  
6 of snow collected at DC (Table 1), mean diurnal HONO emission of  $0.5 \times 10^9$  molecules  $\text{cm}^{-2}$   
7  $\text{s}^{-1}$  is estimated leading to a related HONO mixing ratio of 6.5 pptv (total of 8 pptv together  
8 with NO oxidation). It has to be emphasized that these estimated HONO snow emission  
9 fluxes were derived from values of the HONO/ $\text{NO}_x$  photochemical production ratio observed  
10 in laboratory experiments carried out by flowing zero air through the snow instead of natural  
11 interstitial air of which the chemical composition may be very different.

12 An upper value of the ratio of HONO to  $\text{NO}_x$  mixing ratios often serves as a reference  
13 value to discuss the consistency of HONO mixing ratios (Kleffmann and Wiesen, 2008;  
14 Villena et al., 2011). Steady-state calculations indicate that the HONO/ $\text{NO}_x$  ratio reaches a  
15 maximum value equal to the ratio of HONO to  $\text{NO}_x$  lifetimes ( $\tau_{\text{HONO}}/\tau_{\text{NO}_x}$ ), when it is  
16 assumed that HONO is the sole source of  $\text{NO}_x$ . The measured HONO photolysis rate  
17 constants (see Sect. 2.2) indicate an atmospheric lifetime of HONO at DC ranging from 4.5  
18 min to 24 min at 12:00 and 0:00, respectively. Using OH and  $\text{HO}_2$  concentrations observed by  
19 Kukui et al. (2014), an atmospheric lifetime of  $\text{NO}_x$  ranging from 3 hours at 12:00 to 7 hours  
20 at 0:00 can be estimated. From that, the upper limit of the HONO/ $\text{NO}_x$  ratio at DC would be  
21 close to 0.03 and 0.06 at 12:00 and 0:00, respectively. Using the HONO mixing ratios  
22 simulated when a mean diurnal HONO snow emission of  $0.8 \times 10^9$  molecules  $\text{cm}^{-2} \text{s}^{-1}$  is  
23 considered (Fig. 6) and  $\text{NO}_x$  mixing ratios observed at Concordia (around 200 pptv, Frey et  
24 al., to be submitted), we calculate a mean diurnal HONO/ $\text{NO}_x$  ratio of 0.06. This value  
25 slightly exceeds the maximum steady state HONO/ $\text{NO}_x$  ratio estimated from HONO and  $\text{NO}_x$   
26 photochemical lifetimes. Note, however, that more accurate estimation of the upper limit of  
27 the HONO/ $\text{NO}_x$  ratio should take into account also HONO and  $\text{NO}_x$  vertical distributions  
28 determined by the vertical diffusivity and the conversion of HONO to  $\text{NO}_x$ , as well as by a  
29 possibility of non steady state conditions. As the consideration of these factors may lead to a  
30 higher HONO/ $\text{NO}_x$  ratio, the higher HONO/ $\text{NO}_x$  ratio of about 0.06 cannot be considered as a  
31 strong indication of an error in the simulated HONO mixing ratios derived with an assumed  
32 HONO snow emission of  $0.8 \times 10^9$  molecules  $\text{cm}^{-2} \text{s}^{-1}$ .

33

34 **6. A possible  $\text{HNO}_4$  interference on HONO measurements made with a LOPAP ?**

1 As discussed in the previous section, field measurements of boundary layer HONO  
2 mixing ratios at Concordia in summer (30 pptv) significantly exceed values calculated by  
3 considering a HONO snow source estimated from the observed NO<sub>x</sub> snow source and the  
4 relative abundance of HONO and NO<sub>x</sub> releases observed during snow irradiation BAS  
5 experiments (8 to 12 pptv). As reported in Sect. 2.4, lab experiments conducted with the  
6 LOPAP have shown a possible overestimation of HONO by ~15 pptv due to the presence of  
7 100 pptv of HNO<sub>4</sub>.

8 Although HNO<sub>4</sub> data are not available at Concordia, its presence is very likely since its  
9 atmospheric lifetime with respect to thermal decomposition becomes significant at low  
10 temperatures (lifetime close to 2 h at -20°C, Sanders et al., 2011). Whereas the first  
11 measurements of HNO<sub>4</sub> in Antarctica reported moderate mixing ratios (mean of 25 pptv  
12 observed over a few days in December 2000 at the South Pole, Slusher et al., 2002),  
13 following investigations revealed higher values. First, from 40 pptv in December to 60 pptv  
14 during the second half of November were observed in 2003 at the South Pole (Eisele et al.,  
15 2008). Second, a mean value of 64 pptv (up to 150 pptv) was observed between the ground  
16 and 50 m elevation over the Antarctic plateau (Slusher et al. 2010). These latter values of  
17 HNO<sub>4</sub> mixing ratio together with the above-discussed inconsistencies between simulations  
18 and observations stimulate efforts to investigate a possible interference of HNO<sub>4</sub> on the  
19 LOPAP instrument. Note that given the HNO<sub>4</sub> lifetime with respect to thermal decomposition  
20 of a few hours at -20°C, we don't expect interference during snow experiments conducted at  
21 BAS since HNO<sub>4</sub> initially present in snow collected at DC would have been destroyed during  
22 its storage of a few months at -20°C. Furthermore, production of HNO<sub>4</sub> during the BAS  
23 experiments (Sect. 4) following the release of NO<sub>2</sub> under irradiation of snow is far too slow to  
24 have significantly impacted HONO measurements.

25 Even though laboratory experiences conducted at PSI under certain conditions clearly  
26 showed that there is interference by HNO<sub>4</sub> in HONO measurements made by the LOPAPA  
27 instrument (see Sect. 2.4), the absence of HNO<sub>4</sub> atmospheric data at Dome C hampers any  
28 accurate attempt to correct HONO data from the presence of HNO<sub>4</sub>. Instead, field  
29 experiments were conducted at Concordia heating the air sampled by the LOPAP to thermally  
30 decompose HNO<sub>4</sub>. This air was heated by sucking air through a 8 m long PFA tube covered  
31 with a temperature controlled heating tape and placed in an insulated box. When heating the  
32 tube, the air temperature in the PFA tube was of 37°C leading to a lifetime of HNO<sub>4</sub> with  
33 respect to its thermal decomposition of 3.2 s (Sanders et al., 2011). The experiment was  
34 performed by running the LOPAP for ~ 20 min with and without heating the tube connected

1 to the inlet of the LOPAP. In order to account for possible fast natural change of HONO  
2 mixing ratios the test was repeated three times successively. A systematic drop of HONO  
3 values was observed. Given the applied air sampling flow rate of  $1.78 \text{ L min}^{-1}$  ( $1 \text{ L STP min}^{-1}$ )  
4 <sup>1</sup>), the residence time of the air in the tube is 3.3 s. If attributed to the thermal decomposition  
5 of  $\text{HNO}_4$  during the heating (64% under these working conditions), the mean observed drop  
6 of 5.5 pptv of HONO would correspond to an  $\text{HNO}_4$  artefact of around 9 pptv.

7 This indirect estimation of an overestimation of HONO measurements due to the  
8 presence of  $\text{HNO}_4$  is consistent with experiences conducted at PSI if the presence of 50-100  
9 pptv of  $\text{HNO}_4$  is assumed at Concordia. On the other hand, the difference between observed  
10 and simulated HONO mixing ratios presented in Sect. 5 suggests a mean diurnal  
11 overestimation close to 20 pptv (ranging from 17 pptv around noon to 22 pptv during the  
12 night). In their discussions of the observed levels of  $\text{HO}_x$  radicals, Kukui et al., (2014) found  
13 that the consideration of 30 pptv of HONO is inconsistent with radical observations leading to  
14 about 2 times overestimation of  $\text{RO}_2$  and OH concentrations. Conversely, neglecting the OH  
15 production from HONO leads to an underestimation of radical levels by a factor of 2. Kukui  
16 et al. (2014) showed that a quite fair agreement with OH measurements is achieved with  
17 HONO mixing ratios derived from the 1D modelling with a HONO snow emission flux equal  
18 to about 30% of that of  $\text{NO}_x$ . Finally, though being slightly higher, the best guess of HONO  
19 mixing ratios derived in Sect. 5 for DC (8 to 12 pptv) are in the range of mixing ratios  
20 measurements made at the South Pole using laser-induced fluorescence (6 pptv, Liao et al.,  
21 2006).

## 22

## 23 **7. Conclusions**

24 This second study of HONO conducted in the atmosphere of the East Antarctic plateau  
25 by deploying a LOPAP confirms unexpectedly high mixing ratios close to 30 pptv. A mixing  
26 ratio of 8-12 pptv can be rationalized based on emissions of HONO from snow of  $0.5\text{-}0.8 \times 10^9$   
27 molecules  $\text{cm}^{-2} \text{ s}^{-1}$  derived from studies of the irradiation experiments surface snow collected  
28 at DC and scaled down to the  $\text{NO}_x$  emissions derived from observations made at Concordia  
29 by Frey et al. (to be submitted). Experiments conducted in the field and in the lab to identify  
30 the cause of such a discrepancy point to a possible overestimation of HONO in the range of  
31 10 to 20 pptv due to the important presence of  $\text{HNO}_4$  in this cold atmosphere. An accurate  
32 correction of the HONO data from the presence of  $\text{HNO}_4$  is not yet possible. Further work,  
33 both in the lab to quantify the interference at different levels of  $\text{HNO}_4$  and in the presence of

1 various other species and in the field at Concordia to obtain mixing ratios of HONO and  
2 HNO<sub>4</sub> at the same time are needed.

3

4

5

6 **Acknowledgements.** The OPALE project was funded by the ANR (Agence National de  
7 Recherche) contract ANR-09-BLAN-0226. The measurement of the specific snow area was  
8 developed in the framework of the MONISNOW projet funded by the ANR-11-JS56-005-  
9 01contract. National financial support and field logistic supplies for the summer campaign  
10 were provided by Institut Polaire Français-Paul Emile Victor (IPEV) within programs N° 414,  
11 903, and 1011. M.D. King was supported by NERC NE/F0004796/1 and NE/F010788, NERC  
12 FSF grants 555.0608 and 584.0609. Thanks to our Italian colleagues from Meteo-  
13 Climatological Observatory of PNRA for the meteorological data collected at Concordia.

14

1  
2  
3  
4  
5  
6  
7  
8  
9  
10  
11  
12  
13  
14  
15  
16  
17  
18  
19  
20  
21  
22  
23  
24  
25  
26  
27  
28  
29  
30  
31  
32  
33

**References:**

Arnaud, L., Picard, G., Champollion, N., Dominé, F., Gallet, J.C., Lefebvre, E., Fily, M., and Barnola, J.M.: Measurement of vertical profiles of snow specific surface area with a 1 cm resolution using infrared reflectance: instrument description and validation, *J. of Glaciol.*, 57 (201), 17–29, 2011.

Bartels-Rausch, T., Brigante, M., Elshorbany, Y.F., Ammann, M., D’Anna, B., George, C., Stemmler, K., Ndour, M., and Kleffmann, J. : Humic acid in ice: Photo-enhanced conversion of nitrogen dioxide into nitrous acid, *Atmos. Environ.*, 44, 5443–5450, doi:10.1016/j.atmosenv.2009.12.025, 2010.

Bartels-Rausch, T., Ulrich, T., Huthwelker, T., and Ammann, M.: A novel synthesis of the radiactively labelled atmospheric trace gas peroxyxynitric acid, *Radiochim. Acta*, 99, 1–8, doi:10.1524/ract.2011.1830, 2011.

Bauguitte, S.J.-B., Bloss, W.J., Evans, M.J., Salmon, R.A., Anderson, P.S., Jones, A.E., Lee, J.D., Saiz-Lopez, A., Roscoe, H.K., Wolff, E.W., and Plane, J.M.C.: Summertime NO<sub>x</sub> measurements during the CHABLIS campaign: can source and sink estimates unravel observed diurnal cycles?, *Atmos. Chem. Phys.*, 12(2), 989–1002, doi:10.5194/acp-12-989-2012, 2012.

Beine, H.J., Amoroso, A., Dominé, F., King, M., Nardino, M., Ianniello, A., and France, J. L.: Surprisingly small HONO emissions from snow surfaces at Browning Pass, Antarctica, *Atmos. Chem. Phys.*, 6, 2569–2580, <http://www.atmos-chem-phys.net/6/2569/2006/>, 2006.

Calace, N., Cantafora, E., Mirante, S., Petronio, B. M., and Pietroletti, M.: Transport and modification of humic substances present in Antarctic snow and ancient ice, *J. Environ. Monit.*, 7, 1320-1325, 2005.

Chan, W.H., Nordstrom, R.J., Galvert, J.G., and Shaw, J.H.: An IRFTS spectroscopic study of the kinetics and the mechanism of the reactions in the gaseous system, HONO, NO, NO<sub>2</sub>, H<sub>2</sub>O, *Chem. Phys. Lett.*, 37(3), 441–446, doi:10.1016/0009-2614(76)85010-5, 1976.

1  
2 Chen, G., Davis, D., Crawford, J., Nowak, J.B., Eisele, F., Mauldin, R.L., Tanner, D., Buhr,  
3 M., Shetter, R., Lefer, B., Arimoto, R., Hogan, A., Blake, D.: An investigation of South Pole  
4 HOx chemistry: comparison of model results with ISCAT observations, *Geophys. Res. Lett.*,  
5 28 (19), 3633-3636, 2001.  
6  
7 Chen, G., Davis, D., Crawford, J., Mauldin III, R., Eisele, F., Huey, G., Slusher, D., Tanner,  
8 D., Dibb, J., Buhr, M., Hutterli, M., McConnell, J., Lefer, B., Shetter, R., Blake, D.,  
9 Lombardi, K., and Arnoldy, J. : A reassessment of HOx South Pole chemistry based on  
10 observations recorded during ISCAT 2000, *Atmos. Environ.*, 38(32), 5451–5461,  
11 doi:10.1016/j.atmosenv.2003.07.018, 2004.  
12  
13 Cotter, E.S.N., Jones, A.E., Wolff, E.W., and Bauguitte, S.J.-B.: What controls photochemical  
14 NO and NO<sub>2</sub> production from Antarctic snow? Laboratory investigation assessing the  
15 wavelength and temperature dependence, *J. Geophys. Res.*, 108(D4), 4147,  
16 doi:10.1029/2002JD002602, 2003.  
17  
18 Crowley, J.N., Ammann, M., Cox, R.A., Hynes, R.G., Jenkin, M.E., Mellouki, A., Rossi,  
19 M.J., Troe, J., and Wallington, T.J.: Evaluated kinetic and photochemical data for  
20 atmospheric chemistry: Volume V – heterogeneous reactions on solid substrates, *Atmos.*  
21 *Chem. Phys.*, 10(18), 9059–9223. doi:10.5194/acp-10-9059-2010, 2010.  
22  
23 Davis, D., Nowak, J.B., Chen, G., Buhr, M., Arimoto, R., Hogan, A., Eisele, F., Mauldin, L.,  
24 Tanner, D., Shetter, R., Lefer, B., and McMurry, P. : Unexpected high levels of NO observed  
25 at South Pole, *Geophys. Res. Lett.*, 28(19), 3625–3628, doi:10.1029/ 2000GL012584, 2001.  
26  
27 Dibb, J.E., Arsenault, M., Peterson, M.C., and Honrath, R.E. : Fast nitrogen oxide  
28 photochemistry in Summit, Greenland snow, *Atmos. Environ.*, 36, 2501-2511,  
29 doi:10.1016/S1352-2310(02)00130-9, 2002.  
30  
31 Dibb, J.E., Huey, L.G., Slusher, D.L., and Tanner, D. J.: Soluble reactive nitrogen oxides at  
32 South Pole during ISCAT 2000, *Atmos. Environ.*, 38, 5399–5409, 2004.  
33

1 Eisele, F., Davis, D.D., Helmig, D., Oltmans, S.J., Neff, W., Huey, G., Tanner, Chen, G.,  
2 Crawford, J., Arimoto, R., Buhr, M., J., Mauldin, L., Hutterli, M., Dibb, J., Blake, D.,  
3 Brooks, S.B., Johnson, B., Roberts, J.M., Wang, Y., Tan, D., and Flocke, F. : Antarctic  
4 tropospheric chemistry investigation (ANTCI) 2003 overview, *Atmos. Environ.*, 42(12),  
5 2749–2761, doi:10.1016/j.atmosenv.2007.04.013, 2008.

6

7 Finlayson-Pitts, B.J., Wingen, L.M., Sumner, A.L., Syomin, D., and Ramazan, K.A.: The  
8 heterogeneous hydrolysis of NO<sub>2</sub> in laboratory systems and in outdoor and indoor  
9 atmospheres: An integrated mechanism, *Phys. Chem. Chem. Phys.*, 5, 223–242,  
10 doi:10.1039/b208564j, 2003.

11

12 France, J.L., King, M.D., Frey, M.M., Erbland, J., Picard, G., Preunkert, S., MacArthur, A.,  
13 and Savarino, J.: Snow optical properties at Dome C, Antarctica; implications for snow  
14 emissions and snow chemistry of reactive nitrogen, *Atmos. Chem. Phys.*, 11, 9787-9801,  
15 2011.

16

17 Frey, M.M., Brough, N., France, J.L., Anderson, P.S., Traulle, O., King, M.D., Jones, A.E.,  
18 Wolff, E.W., and Savarino, J.: The diurnal variability of atmospheric nitrogen oxides (NO and  
19 NO<sub>2</sub>) above the Antarctic Plateau driven by atmospheric stability and snow emissions, *Atmos.*  
20 *Chem. Phys.*, 13, 3045–3062, doi:10.5194/acp-13-3045-2013, 2013.

21

22 Frey, M.M., Roscoe, H.K., Kukui, S., Savarino, J., France, J.L., King, M.D., Legrand, M., and  
23 Preunkert, S.: Atmospheric nitrogen oxides (NO and NO<sub>2</sub>) at Dome C, East Antarctica, during  
24 the OPAL campaign, to be submitted.

25

26 Gaffney, J.S., Marley, N.A., and Cunningham, M.M.: Measurement of the absorption  
27 constants for nitrate in water between 270 and 335 nm, *Environ. Sci. Technol.*, 25, 207–209,  
28 1992.

29

30 Gallet, J.-C., Dominé, F., Arnaud, L., Picard, G., and Savarino, J.: Vertical profile of the  
31 specific surface area and density of the snow at Dome C and on a transect to Dumont  
32 D’Urville, Antarctica – albedo calculations and comparison to remote sensing products, *The*  
33 *Cryosphere*, 5, 631–649, doi:10.5194/tc-5-631-2011, 2011.

34

1 Gallée, H. and Gorodetskaya, I.: Validation of a limited area model over Dome C, Antarctic  
2 Plateau, during winter, 34, 61–72, *Clim. Dyn.*, doi:10.1007/s00382-008-0499-y, 2008.  
3  
4 Gallée, H., Preunkert, S., Jourdain, B., Argentini, S., Frey, M., Genthon, C., Pietroni, I.,  
5 Casasanta, G., and Legrand, M. : Characterization of the boundary layer at Dome C during  
6 OPALE, *Atmos. Chem. Phys.*, to be submitted.  
7  
8 George, C., Streckowski, R.S., Kleffmann, J., Stemmler, K., and Ammann, M.: Photoenhanced  
9 uptake of gaseous NO<sub>2</sub> on solid organic compounds: a photochemical source of HONO,  
10 *Faraday Discuss.*, 130, 195–211, 2005.  
11  
12 Grannas, A.M., Jones, A.E., Dibb, J., Ammann, M., Anastasio, C., Beine, H.J., Bergin, M.,  
13 Bottenheim, J., Boxe, C.S., Carver, G., Chen, G., Crawford, J.H., Domine', F., Frey, M.M.,  
14 Guzmán, M.I., Heard, D.E., Helmig, D., Hoffmann, M.R., Honrath, R.E., Huey, L.G.,  
15 Hutterli, M., Jacobi, H.W., Klán, P., Lefer, B., McConnell, J., Plane, J., Sander, R., Savarino,  
16 J., Shepson, P.B., Simpson, W.R., Sodeau, J.R., von Glasow, R., Weller, R., Wolff, E.W., and  
17 Zhu, T.: An overview of snow photochemistry: evidence, mechanisms and impacts, *Atmos.*  
18 *Chem. Phys.*, 7, 4329–4373, <http://www.atmos-chem-phys.net/7/4329/2007/>, 2007.  
19  
20 Gutzwiller, L., Arens, F., Baltensperger, U., Gäggeler, H.W., and Ammann, M.: Significance  
21 of semivolatile diesel exhaust organics for secondary HONO formation, *Environ. Sci.*  
22 *Technol.*, 36, 677-682, doi:10.1021/es015673b, 2002.  
23  
24 Heland, J., Kleffmann, J., Kurtenbach, R., and Wiesen, P. : A new instrument to measure  
25 gaseous nitrous acid (HONO) in the atmosphere, *Environ. Sci. Technol.*, 35(15), 3207-3212,  
26 doi:10.1021/es000303t, 2001.  
27  
28 Hudson, S.R., Warren, S.G., Brandt, R.E., Grenfell, T.C., and Six, D. : Spectral bidirectional  
29 reflectance of Antarctic snow: Measurements and parameterization, *J. Geophys. Res.*, 111,  
30 D18106, doi:10.1029/2006JD007290, 2006.  
31  
32 Jones, A.E., Weller, R., Wolff, E.W., and Jacobi, H.-W.: Speciation and rate of  
33 photochemical NO and NO<sub>2</sub> production in Antarctic snow, *Geophys. Res. Lett.*, 27(3), 345–  
34 348, 2000.



1  
2 Kerbrat, M., Legrand, M., Preunkert, S., Gallée, H., and Kleffmann, J.: Nitrous Acid at  
3 Concordia on the East Antarctic Plateau and its transport to the coastal site of Dumont  
4 d'Urville, *J. Geophys. Res.*, 117, D08303, doi:10.1029/2011JD017149, 2012.  
5  
6 Kirchstetter, T.W., Harley, R.A., and Littlejohn, D.: Measurement of nitrous acid in motor  
7 vehicle exhaust, *Environ. Sci. Technol.*, 30, 2843-2849, 10.1021/es960135y, 1996.  
8  
9 Kleffmann, J., Heland, J., Kurtenbach, R., Lorzer, J., and Wiesen, P.: A new instrument  
10 (LOPAP) for the detection of nitrous acid (HONO), *Environ. Sci. Pollut. Res.*, (Sp. Iss. 4),  
11 48–54, 2002.  
12  
13 Kleffmann, J., and Wiesen, P.: Technical Note: Quantification of interferences of wet  
14 chemical HONO LOPAP measurements under simulated polar conditions, *Atmos. Chem.*  
15 *Phys.*, 8, 6813–6822, www.atmos-chem-phys.net/8/6813/2008/, 2008.  
16  
17 Kokhanovsky, A.A., and Zege, E.P.: Scattering optics of snow, *Appl. Optics*, 43, 1589–1602,  
18 2004.  
19  
20 Kukui, A., Legrand, M., Ancellet, G., Gros, V., Bekki, S., Sarda-Estève, R., Loisil, R., and  
21 Preunkert, S.: Measurements of OH and RO<sub>2</sub> radicals at the coastal Antarctic site of Dumont  
22 d'Urville (East Antarctica) in summer, *J. Geophys. Res.*, doi:10.1029/2012JD017614, 2012.  
23  
24 Kukui, A., Legrand, M., Preunkert, S., Frey, M., Loisil, R., Gil Roca, J., Jourdain, B., King,  
25 M., France, J., and Ancellet, G.: OH and RO<sub>2</sub> measurements at Dome C, East Antarctica,  
26 *Atmos. Chem. Phys. Discuss.*, 14, 14999-15044, 2014.  
27  
28 Kurtenbach, R., Becker, K.H., Gomes, J.A.G., Kleffmann, J., Lorzer, J.C., Spittler, M.,  
29 Wiesen, P., Ackermann, R., Geyer, A., and Platt, U.: Investigations of emissions and  
30 heterogeneous formation of HONO in a road traffic tunnel, *Atmos. Environ.*, 35, 3385-3394,  
31 10.1016/s1352- 2310(01)00138-8, 2001.  
32

1 Legrand M., Preunkert, S., Jourdain, B., Gallée, H., Goutail, F., Weller, R., and Savarino, J.:  
2 Year round record of surface ozone at coastal (Dumont d'Urville) and inland (Concordia)  
3 sites in East Antarctica, *J. Geophys. Res.*, 114, D20306, doi:10.1029/2008JD011667, 2009.  
4

5 Legrand, M., Preunkert, S., Jourdain, B., Guilhermet, J., Faïn, X., Alekhina, I., and Petit, J.R. :  
6 Water-soluble organic carbon in snow and ice deposited at Alpine, Greenland, and Antarctic  
7 sites: A critical review of available data and their atmospheric relevance, *Clim. Past*, 9, 2195-  
8 2211, doi:10.5194/cp-9-2195-2013, 2013.  
9

10 Li, X., Rohrer, F., Hofzumahaus, A., Brauers, T., Häsel, R., Bohn, B., Broch, S., Fuchs, H.,  
11 Gomm, S., Holland, F., Jäger, J., Kaiser, J., Keutsch, F. N., Lohse, I., Lu, K., Tillmann, R.,  
12 Wegener, R., Wolfe, G. M., Mentel, T. F., Kiendler-Scharr, A., and Wahner, A.: Missing  
13 Gas-Phase Source of HONO Inferred from Zeppelin Measurements in the Troposphere,  
14 *Science*, 344, 292-296, 2014.  
15

16 Liao, W., Case, A.T., Mastromarino, J., Tan, D., and Dibb, J.E. : Observations of HONO by  
17 laser-induced fluorescence at the South Pole during ANTCI 2003, *Geophys. Res. Lett.*, 33,  
18 L09810, doi:10.1029/2005GL025470, 2006.  
19

20 Mauldin, R.L., Eisele, F.L., Tanner, D.J., Kosciuch, E., Shetter, R., Lefer, B., Hall, S.R.,  
21 Nowak, J.B., Buhr, M., Chen, G., Wang, P., and Davis, D. : Measurements of OH, H<sub>2</sub>SO<sub>4</sub>,  
22 and MSA at the South Pole during ISCAT, *Atmos. Environ.*, 28, 3629-3632, 2001a.  
23

24 Mauldin III, R.L., Eisele, F.L., Cantrell, C.A., Kosciuch, E., Ridley, B.A., Lefer, B., Tanner,  
25 D.J., Nowak, J.B., Chen, G., Wang, L., and Davis, D. : Measurements of OH aboard the ASA  
26 P-3 during PEM-Tropics B., *J. Geophys. Res.*, 106, 32,657-32,666, 2001b.  
27

28 Meusinger, C., Berhanu, T.A., Erbland, J., Savarino, J., and Johnson, M.S. : Laboratory Study  
29 of Nitrate Photolysis in Antarctic Snow, Part 1: Observed Quantum Yield, Domain of  
30 Photolysis and Secondary Chemistry, *J. Chem. Phys.*, 140, 244305, 2014.  
31

32 Preunkert S., Ancellet, G., Legrand, M., Kukui, A., Kerbrat, M., Sarda-Estève, R., Gros, V.,  
33 and Jourdain, B.: Oxidant Production over Antarctic Land and its Export (OPALE) project:

1 An overview of the 2010-2011 summer campaign, *J. Geophys. Res.*,  
2 doi:10.1029/2011JD017145, 2012.  
3

4 Regimbal, J., and Mozurkewich, M.: Peroxynitric acid decay mechanisms and kinetics at low  
5 pH, *J. Phys. Chem. A*, 101, 8822–8829, 1997.  
6

7 Sander, S.P., and Peterson, A.E.: Kinetics of the reaction  $\text{HO}_2 + \text{NO}_2 + \text{M} \rightarrow \text{HO}_2\text{NO}_2 + \text{M}$ , *J.*  
8 *Phys. Chem.*, 88, 166-1571, 1984.  
9

10 Sander, S.P., J. Abbatt, J.R. Barker, J.B. Burkholder, R.R. Friedl, D.M. Golden, R.E. Huie, C.  
11 E. Kolb, M.J. Kurylo, G.K. Moortgat, V.L. Orkin and P.H. Wine : "Chemical Kinetics and  
12 Photochemical Data for Use in Atmospheric Studies, Evaluation No. 17," JPL Publication 10  
13 June 2011, Jet Propulsion Laboratory, Pasadena, <http://jpldataeval.jpl.nasa.gov>, 2011.  
14

15 Slusher, D.L., Huey, L.G., Tanner, D.J., Chen, G., Davis, D.D., Buhr, M., Nowak, J.B.,  
16 Eisele, F., Kosciuch, E., Mauldin, R.L., Lefer, B.L., Shetter, R.E., and Dibb, J.E.:  
17 Measurements of pernitric acid at the South Pole during ISCAT 2000, *Geophys. Res. Lett.*,  
18 29, 2011, doi:10.1029/2002GL015703, 2002.  
19

20 Slusher, D.L., Neff, W.D., Kim, S., Huey, L.G., Wang, Y., Zeng, T., Tanner, D.J., Blake, D.  
21 R., Beyersdorf, A., Lefer, B.L., Crawford, J.H., Eisele, F.L., Mauldin, R.L., Kosciuch, E.,  
22 Buhr, M.P., Wallace, H.W., and Davis, D.D.: Atmospheric chemistry results from the ANTCI  
23 2005 Antarctic plateau airborne study, *J. Geophys. Res. Atmos.*, 115, D07304,  
24 doi:10.1029/2009JD012605, 2010.  
25

26 Ulrich, T., Ammann, M., Leutwyler, S., and Bartels-Rausch, T.: The adsorption of  
27 peroxynitric acid on ice between 230 K and 253 K, *Atmos. Chem. Phys.*, 12, 1833-1845,  
28 10.5194/acp-12-1833-2012, 2012.  
29

30 Villena, G., Wiesen, P., Cantrell, C.A., Flocke, F., Fried, A., Hall, S.R., Hornbrook, R.S.,  
31 Knapp, D., Kosciuch, E., Mauldin III, R.L., McGrath, J.A., Montzka, D., Richter, D.,  
32 Ullmann, K., Walega, J., Weibring, P., Weinheimer, A., Staebler, R.M., Liao, J., Huey, L.G.,  
33 and Kleffmann, J. : Nitrous acid (HONO) during polar spring in Barrow, Alaska: A net source  
34 of OH radicals?, *J. Geophys. Res.*, 116, D00R07, doi:10.1029/2011JD016643, 2011.



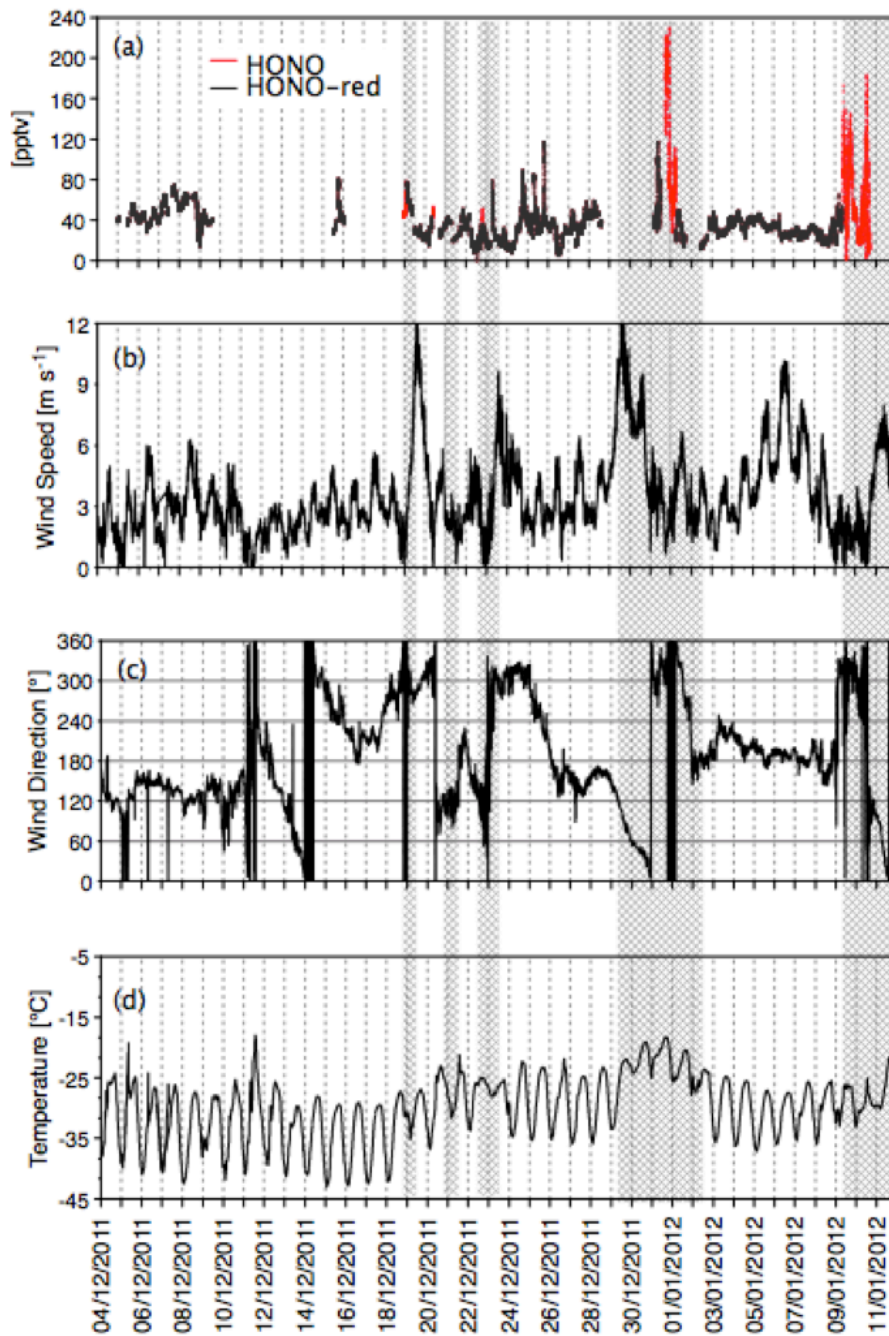
1  
2  
3  
4  
5  
6  
7  
  
8  
9  
10  
11  
12  
13  
14  
15

**Table 1.** Results of irradiation experiments performed at the BAS laboratory on three different surface snows collected at DC. S1 and S2 are upper surface snows collected between 0 and 1 cm, S3 is the surface snow collected between 0 and 12 cm depth. The acidity is calculated by checking the balance between anions and cations (see Sect. 2.2). DL refers to detection limit and N.C. means non-calculated value.

Snow type	Date in 2013	Wavelengths $\lambda >$	T (°C)	HONO (pptv)	NO <sub>x</sub> (pptv)	HONO/NO <sub>x</sub>	NO <sub>3</sub> <sup>-</sup> (ppb)	H <sup>+</sup> (μEq L <sup>-1</sup> )
S1	23 Jan	295 nm	-15	117 ± 5	137 ± 20	0.85 ± 0.1	1428	29.4
S1	24 Jan	295 nm	-15.5	120 ± 3	129 ± 16	0.93 ± 0.1	1428	29.4
S1	24 Jan	320 nm	-16	47 ± 1	67 ± 12	0.70 ± 0.1	1428	29.4
S1	24 Jan	385 nm	-16	< 3	< DL	N.C.	1428	29.4
S2	23 Apr	295 nm	-13	124 ± 1	162 ± 14	0.77 ± 0.1	1344	24.0
S2	23 Apr	295 nm	-22.5	86 ± 3	167 ± 40	0.52 ± 0.1	1344	24.0
S2	23 Apr	295 nm	-34	56 ± 1	210 ± 50	0.27 ± 0.2	1344	24.0
S3	25 Apr	295 nm	-21	15 ± 2	47 ± 27	0.32 ± 0.15	157	4.0

1 **Figures**

2



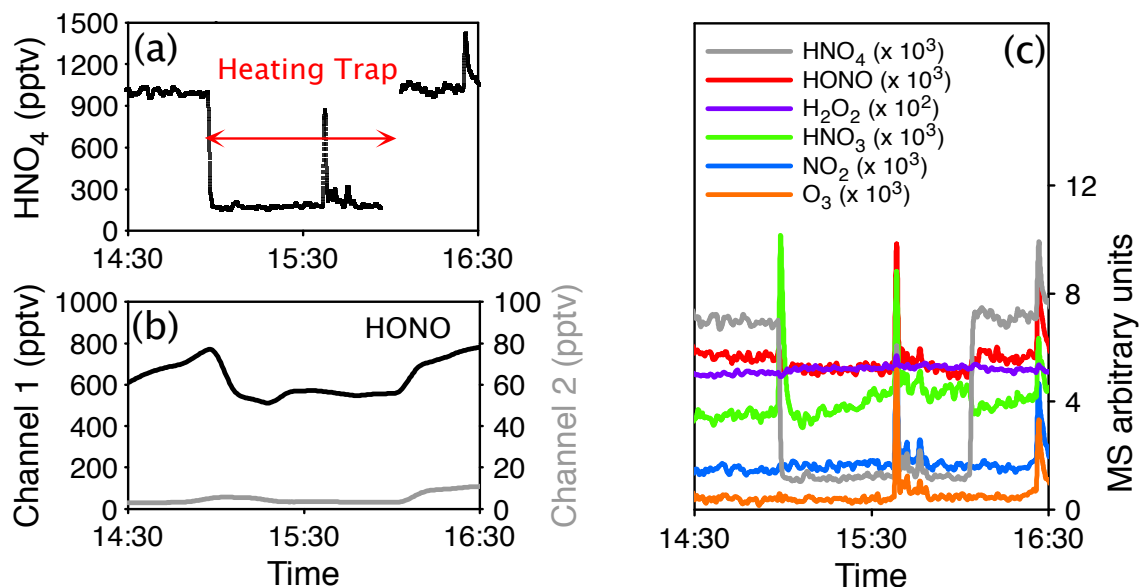
3

4

5 **Fig. 1.** Summer 2011/2012 time series of HONO mixing ratios (1 min average) (a), wind  
6 conditions (b and c) and temperatures (d) at Concordia. Red points of the HONO record refer  
7 to time periods during which contamination from the station was possible with the wind was  
8 blowing from North (from 10°W to 60°E sector, see Sect. 2.2). Grey backgrounds indicate  
9 time period of overcast weather.

10

1



2

3

4

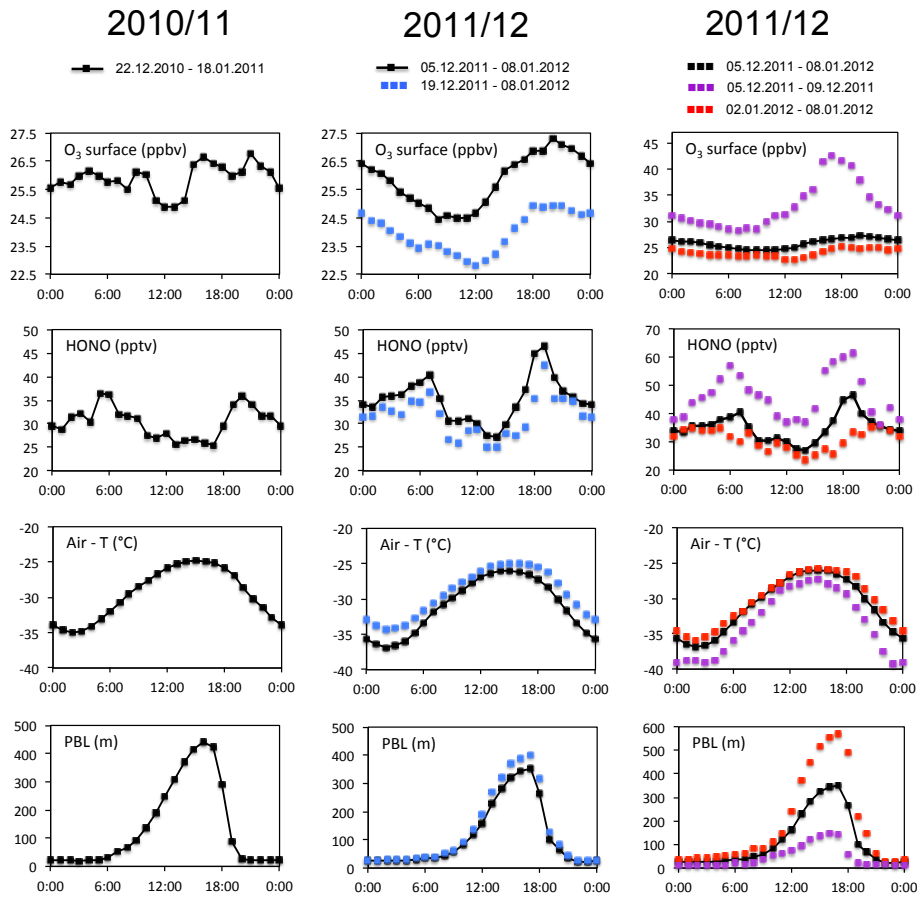
5

6 **Fig. 2.** The experiment carried out at the PSI laboratory in view to investigate the interference  
 7 of HNO<sub>4</sub> on HONO measurements made with the LOPAP deployed during the two Concordia  
 8 campaigns. Left: Time traces of HNO<sub>4</sub> (top) and of the two LOPAP channels (bottom). Time  
 9 at which the heating trap was activated is shown with a red horizontal arrow. Right:  
 10 Intensities of NO<sub>2</sub>, HONO, HNO<sub>3</sub>, HNO<sub>4</sub>, O<sub>3</sub>, and H<sub>2</sub>O<sub>2</sub> traces as detected by the mass  
 11 spectrometer (see Sect. 2.4). Heating the gas mixture to 100°C leads to a sharp decrease in  
 12 HNO<sub>4</sub> and a small increase of HNO<sub>3</sub> intensities. O<sub>3</sub> and H<sub>2</sub>O<sub>2</sub> remain stable whereas a very  
 13 small decrease of HONO is detectable.

14

15

1



2

3

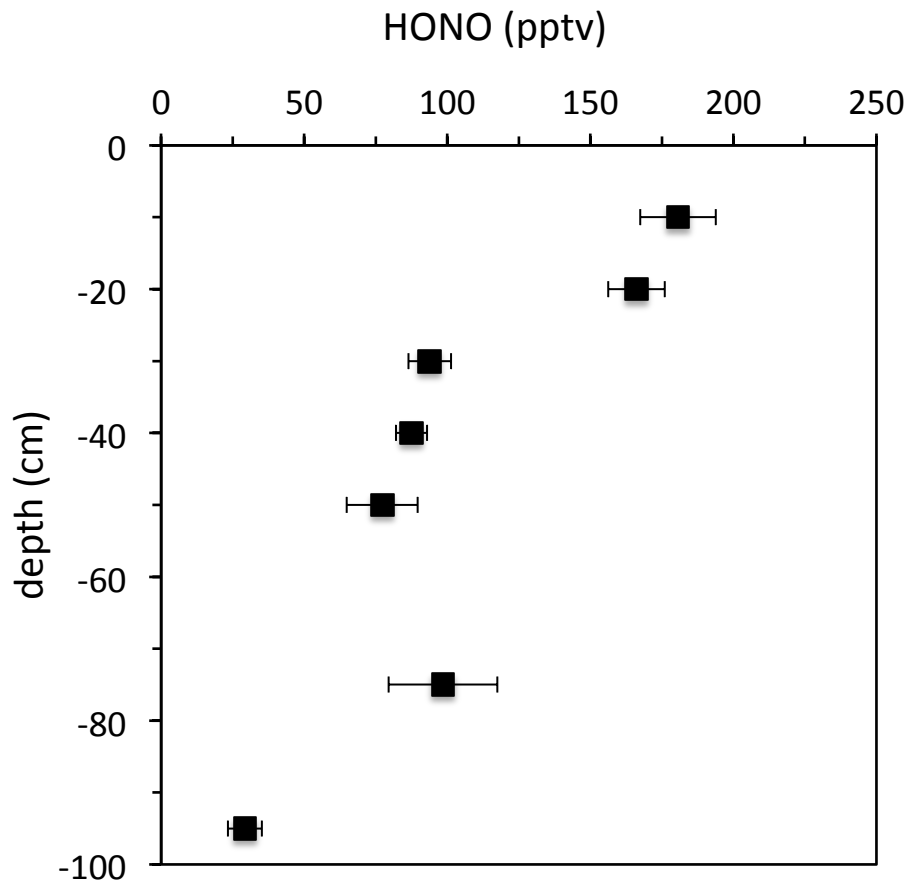
4 **Fig. 3.** Left and central: From top to bottom, diurnal changes of surface ozone mixing ratio,  
 5 HONO mixing ratio, air temperature and PBL height simulated by the MAR model (see Sect.  
 6 5) at Concordia over the entire period of measurements in 2010/2011 (left) and 2011/20112  
 7 central (black dots). The blue dots reported for the 2011/2012 summer correspond to the  
 8 period between December 19<sup>th</sup> 2011 and January 8<sup>th</sup> 2012. Right: Same as left and central but  
 9 for the entire 2011/2012 period (black dots), at the beginning (early December, violet dots)  
 10 and the end (red dots) of the period. Note the use of different vertical scales for right  
 11 compared to left and central panels.

12

13



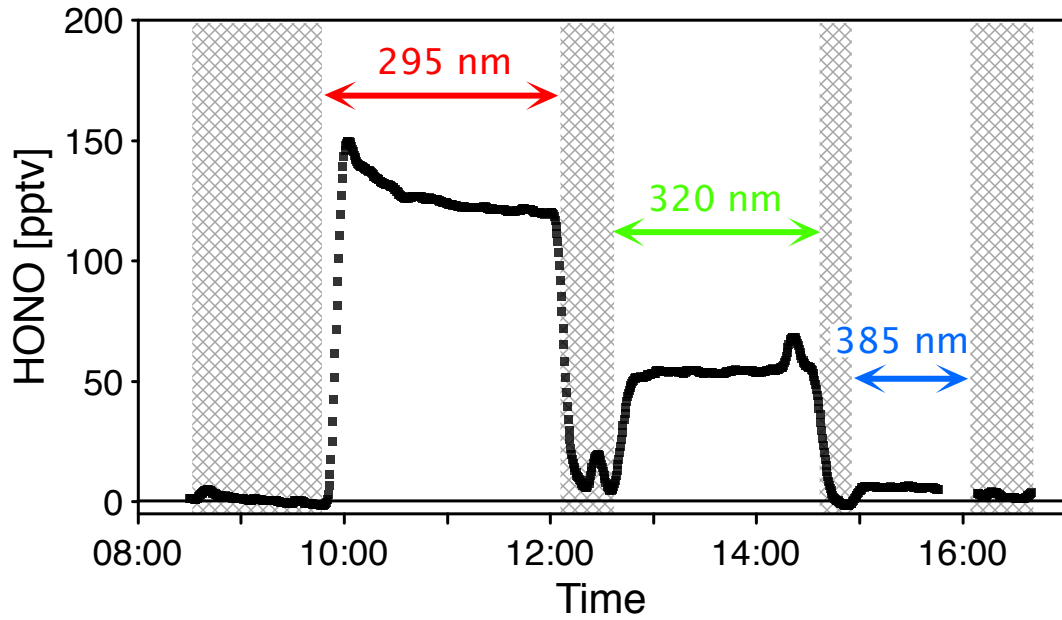
1  
2



3  
4  
5  
6  
7  
8  
9

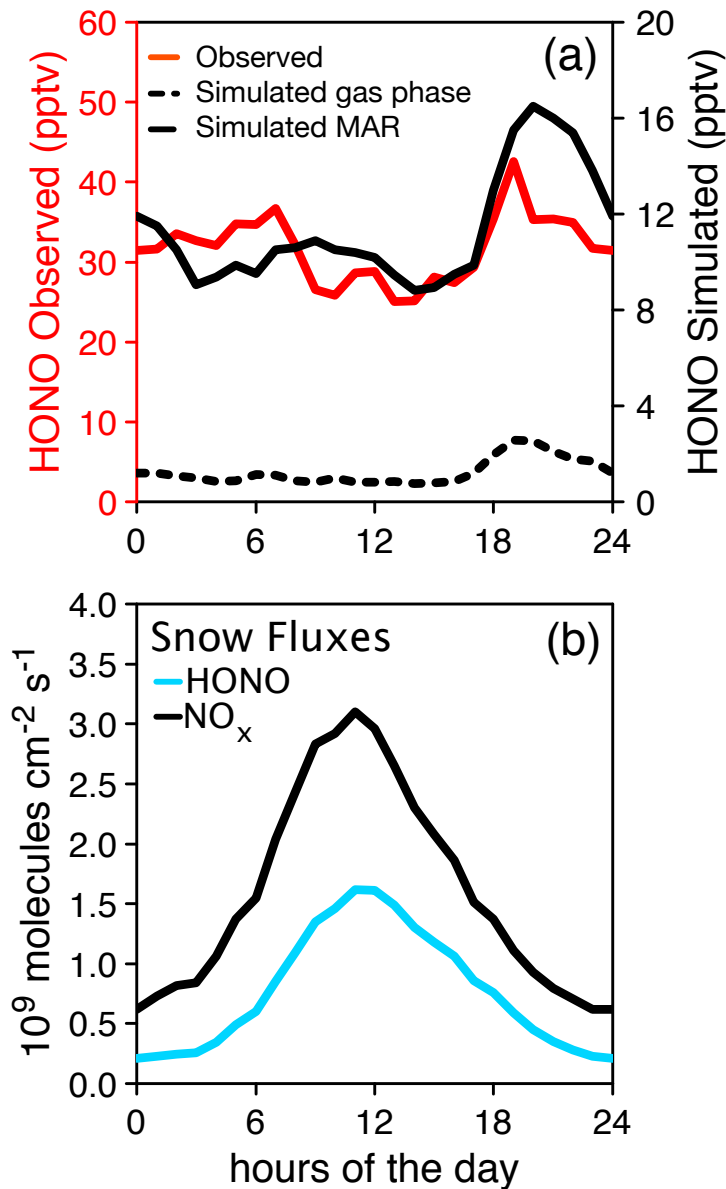
**Fig. 4.** Firn air mixing ratios of HONO down to 1 m depth measured at DC at 13 January 2012.

1  
2



3  
4  
5  
6  
7  
8  
9  
10

**Fig. 5.** Photochemical release of HONO from a surface snow collected at DC when irradiating it at a temperature of  $-16^{\circ}\text{C}$  (see Table 1) and inserting filters with cut-on points at 295 nm, 320 nm, and 385 nm on the Xenon-arc lamp (see Sect. 4). Vertical grey bands correspond to periods over which the lamp was switched off.



1  
 2  
 3 **Fig. 6.** Top : Measured (red line) versus simulated (black lines) (see Sect. 5) diurnal cycles of  
 4 HONO mixing ratio at 1 m height. Note the use of a different vertical scale for observations  
 5 (left) and simulations (right). The black dashed line is the simulation made when considering  
 6 only the gas phase production of HONO from NO (without snow emissions). Bottom :  
 7 Diurnal NO<sub>x</sub> snow source derived from field observations at Concordia (Frey et al., to be  
 8 submitted) together with an estimated emission of HONO from snow based on laboratory  
 9 snow irradiation experiments (see Sect. 4).

10